Computer simulation of the discharge of metal electrodes in batteries with solid electrolytes

Gennady I. Ostapenko[a,*], Sergey N. Antonov[b]

[a]*Institute of Radio Engineering and Electronics, Russian Academy of Sciences, Ul'anovsk Division, 48 Goncharov Str., 432011 Ul'anovsk, Russia*
[b]*Ul'anovsk State Engineering University, 32 Severny Venets Str., 432027 Ul'anovsk, Russia*

Abstract

The computer simulation of the dissolution during discharge of silver electrodes in batteries and other devices with various silver-conducting solid electrolytes was carried out. The model of the pseudo-porous electrode represents small silver spheres, distributed in a solid electrolyte matrix. Various parameters simulated were: diameter of silver particles, silver to electrolyte relationship within the electrode, thickness of the electrode, conductivity of the electrolyte, discharge current and thickness of the separator. Calculated distribution of current in the electrode and the discharge curves at various parameters were obtained. A comparison of the calculated and experimental discharge curves was carried out. The good correspondence of these curves testifies to adequacy of the surveyed model of the dissolution of metal electrode for devices with solid electrolytes. Optimal parameters of the electrode are recommended depending on the use of these devices with solid electrolytes. © 2001 Elsevier Science B.V. All rights reserved.

Keywords: Solid electrolyte batteries; Porous electrodes; Computer simulation

1. Introduction

Batteries and other devices using solid electrolytes can function at zero gravity, under high accelerations and over a wide range of temperature. Such devices have practically unlimited prospects for miniaturization. So, they have excellent prospects for general application in cosmic and military equipment. Usually, one of the electrodes of the solid-state battery is a soluble (during discharge) metal electrode [1]. Frequently, metal electrodes are prepared by the pressing of metal and solid electrolyte powders [2,3]. This is done to lower electrode polarization. In such electrodes, the metal particles are distributed in the solid electrolyte matrix and these electrodes can be viewed as pseudo-porous.

The effective area of the porous electrode is distributed throughout its volume. All parts within the electrode volume are not equally accessible for electrochemical processes, therefore the intensity of the electrode discharge is unequal within the electrode. The theory of porous electrodes gives the current density and potential distribution within the electrode volume or thickness.

In the present work, computer simulation were carried out of electrochemical dissolution of the pseudo-porous silver electrode for the device with the solid electrolyte, depending on the diameter of the silver particles, silver: electrolyte relation in the electrode, thickness of the electrode, conductivity of the electrolyte, discharge current and thickness of the separator.

2. Formulation

2.1. Description of the electrode model

One of the first major theoretical investigations of the porous electrode was carried out by Stender [4]. Then Coleman [5], Daniel-Bek [6] and Frumkin [7] carried out the quantitative calculations of the current distribution. The problems of the porous electrode simulation by means of electrical elements were surveyed fully by Euler [8–10].

For simplification, the two-phase porous electrode is considered usually as a pseudo-homogeneous medium. This medium has a certain electrical resistance R, which includes ohmic resistance R_Ω and polarization resistance R^η.

The resistance R_Ω is the total electronic resistance of the metal electrode R^m, ionic resistances in the electrolyte pores

---

* Corresponding author.
E-mail address: ufire@mv.ru (G.I. Ostapenko).

R^e and in the separator R^s. The nonlinear resistance R^η is stipulated by polarization phenomenon at the metal/electrolyte interface. Current i_n at any site in the porous electrode is inversely proportional to the complete resistance R_n during current flow through this site.

For simulation, the porous electrode is divided conditionally into N sections, which run connected to an external current source AB, as shown in Fig. 1. The following series of linear equations can be deduced:

$$R_1 = NR^m + R^e + R_1^\eta + R^s$$

$$R_2 = (N-1)R^m + 2R^e + R_2^\eta + R^s$$

$$R_n = (N-n+1)R^m + nR^e + R_n^\eta + R^s$$

$$R_N = R^m + NR^e + R_N^\eta + R^s$$

$$\frac{1}{R} = \sum_{n=1}^{n=N} \frac{1}{R_n}$$

$$\Delta\varphi_{AB} = IR$$

$$I = i_1 + i_2 + \cdots + i_n + \cdots + i_N$$

where $\Delta\varphi_{AB}$ is voltage drop between points A and B, i.e. electrode polarization; I the overall current through the electrode. This set of simultaneous equations was solved by the Gauss method [11].

2.2. Operating conditions and physical parameters

The effective conductivity of porous metal and of porous electrolyte can be calculated as the product of conductivity of the material and some coefficient $K(P)$, which depends on the porosity of the material (Table 1).

The polarization resistance is calculated as

$$R_n^\eta = \frac{\eta_n}{i_n S_n}$$

where S_n is the effective area of metal/electrolyte interface in section n; η_n an overvoltage in section n at current flow i_n. The interrelation $\eta = f(i)$ is determined from the polarization curve of the metal/electrolyte interface.

The electrode material is represented spherical silver particles, distributed in the solid electrolyte matrix. The electrode is a disc with a diameter of 12 mm. The electrode is arbitrarily divided into 20 sections. The polarization curve of the Ag/Ag$_4$RbI$_5$ interface [13] is utilized for the simulation of silver electrodes with other silver-conducting solid electrolytes (Ag$_6$WO$_4$I$_4$), since silver dissolution is reduced by crystallizing effects [13,14] and does not depend on the nature of the solid electrolyte. Tables 2 and 3 show the parameters used in the simulation.

2.3. Background of the algorithmic approach

At the moment of current application, the intensity of discharge in the sections is distributed within the electrode thickness according to a primary distribution [18,19], i.e. is caused only by ohmic resistance R_Ω. Then there is a redistribution of intensity of discharge owing to the origination of polarization resistance R^η and then occurs a secondary distribution of current.

The calculation of the secondary distribution in each section is carried out without reference to the secondary distribution in subsequent sections, which for the present are not known, since the polarization resistance and current in the sections are interdependent. Therefore, secondary distribution is determined by the method of successive

Table 1
Coefficient $K(P)$ which characterizes conductivity of porous bodies vs. porosity P [12]

P	0.9	0.8	0.7	0.6	0.5	0.4	0.3	0.2	0.1	0.0
$K(P)$	0.008	0.033	0.058	0.14	0.222	0.368	0.515	0.687	0.847	1.000

Table 2
Physical parameters

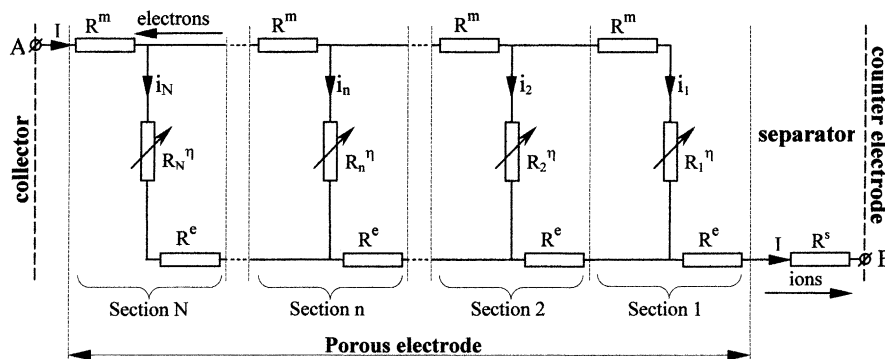| Parameter	Characteristics
Solid electrolytes	Ionic conductivity (S cm^{-1})
Ag$_4$RbI$_5$	2×10^{-1} [15]
Ag$_6$WO$_4$I$_4$	2.3×10^{-2} [16]
Density of electrolyte	5 g cm^{-3} [17]
Density of silver	10.5 g cm^{-3}
Conductivity of silver	6.25×10^9 S cm^{-1}

Fig. 1. Equivalent circuit of the porous electrode. Refer text for notations.

Table 3
Electrode parameters

Electrode number (EN)	Electrode thickness (mm)	Overall current (mA)	Silver to electrolyte (weight ratio)	Electrolyte type	Diameter of silver particles (μm)	Separator thickness (mm)
1	0.5	10	1:0.5	Ag_4RbI_5	2.5	0.5
2	0.2	10	1:0.5	Ag_4RbI_5	2.5	0.5
3	1.0	10	1:0.5	Ag_4RbI_5	2.5	0.5
4	0.5	5	1:0.5	Ag_4RbI_5	2.5	0.5
5	0.5	50	1:0.5	Ag_4RbI_5	2.5	0.5
6	0.5	10	1:0.2	Ag_4RbI_5	2.5	0.5
7	0.5	10	1:1.0	Ag_4RbI_5	2.5	0.5
8	0.5	10	1:0.5	$Ag_6WO_4I_4$	2.5	0.5
9	0.5	10	1:0.5	Ag_4RbI_5	0.5	0.5
10	0.5	10	1:0.5	Ag_4RbI_5	5.0	0.5
11	0.5	10	1:0.5	Ag_4RbI_5	2.5	0.1
12	0.5	10	1:0.5	Ag_4RbI_5	2.5	5.0

approximations. Such an iterative process has a rapid convergence. The calculations stop when the discrepancy of distribution between current and those from previous calculation cycles does not exceed 0.1%.

The metal is dissolved electrochemically at discharge. Therefore metal quantity, the radius and area of metal particles decrease in time. For simplification of the simulation, the calculation of the intensity of discharge in the sections is carried through time intervals $\Delta t_i = t_i - t_{i-1}$, which are selected arbitrarily, according to the theoretical electrical capacity of the electrode and the required accuracy. This approach assumes an invariance of currents within sections during the time interval between t_i and t_{i-1}. Thus, the calculation of current redistribution with time is reduced to a definition of the stationary secondary current distribution at various instants considering the working area changes of the electrode sections with time.

3. Experimental

The solid electrolyte Ag_4RbI_5 was prepared by the method described in [15]. Material for the electrodes was prepared by mixing silver and the solid electrolyte powders (the weight ratio Ag:Ag_4RbI_5 was 1:0.5) or silver, the solid electrolyte and carbon (the weight ratio Ag:Ag_4RbI_5:C was 1:0.5:0.02). The average diameter of silver particles was about 2.5 μm.

Cells of the type: positive collector, investigated electrode/separator/counter electrode were prepared in dry air atmosphere (dehydrator P_2O_5) by sequential pressing under a pressure of 2.2×10^8 Pa:

- Ni foil (as collector);
- powder of investigated electrode material;
- Ag_4RbI_5 powder (as separator);
- Ag foil (as counter electrode).

The cell diameter was 12 mm. The separator thickness was 0.5 mm. A silver wire reference electrode of 0.2 mm

diameter was positioned inside the electrolyte. The clamping pressure applied to the cell was approximately 3×10^6 Pa.

Before measurements began, the cell was annealed for several hours at 140°C. Polarizations of the cells were made with the P-5848 potentiostat (manufacturer: Gomel Instrument Plant, Russia) at room temperature under a current of 10 mA. The voltage $\Delta\varphi$ was measured between the investigated and the reference electrodes.

4. Results and discussion

In Fig. 2 the calculated current distribution within some electrodes is shown. On the ordinate axis, the current flow in the electrode sections is shown. On the abscissa axis the distance from the frontal electrode surface to the interior is shown. The theoretical efficiency is indicated on the curves. Fig. 3 shows the calculated and experimental discharge curves of the electrodes.

As it is shown on Fig. 2, the electrode frontal sections are discharged mainly at the beginning. Then the discharge extends deep into the electrode and at the end, is near the collector.

In Fig. 2a, d and e the dependence of current distribution on overall current quantity I is shown. As it is shown by these figures, the current distribution depends considerably on I, while the non-uniformity of distribution increases with increase of I. The polarization resistance R_n^{η} decreases with section current i_n increase. The electrode polarization $\Delta\varphi$ increases (Fig. 3a, d and e) as I increases.

In Fig. 2a–c the dependence of current distribution on electrode thickness is shown. These figures show that the non-uniformity of current distribution increases with increase of electrode thickness. This is possible to explain by an increase of the electrode ionic resistance. Increase of electrode polarization with decreasing of electrode thickness (Fig. 2a–c) is an interesting effect. However, a thin electrode contains less silver particles than the thick one. Therefore,
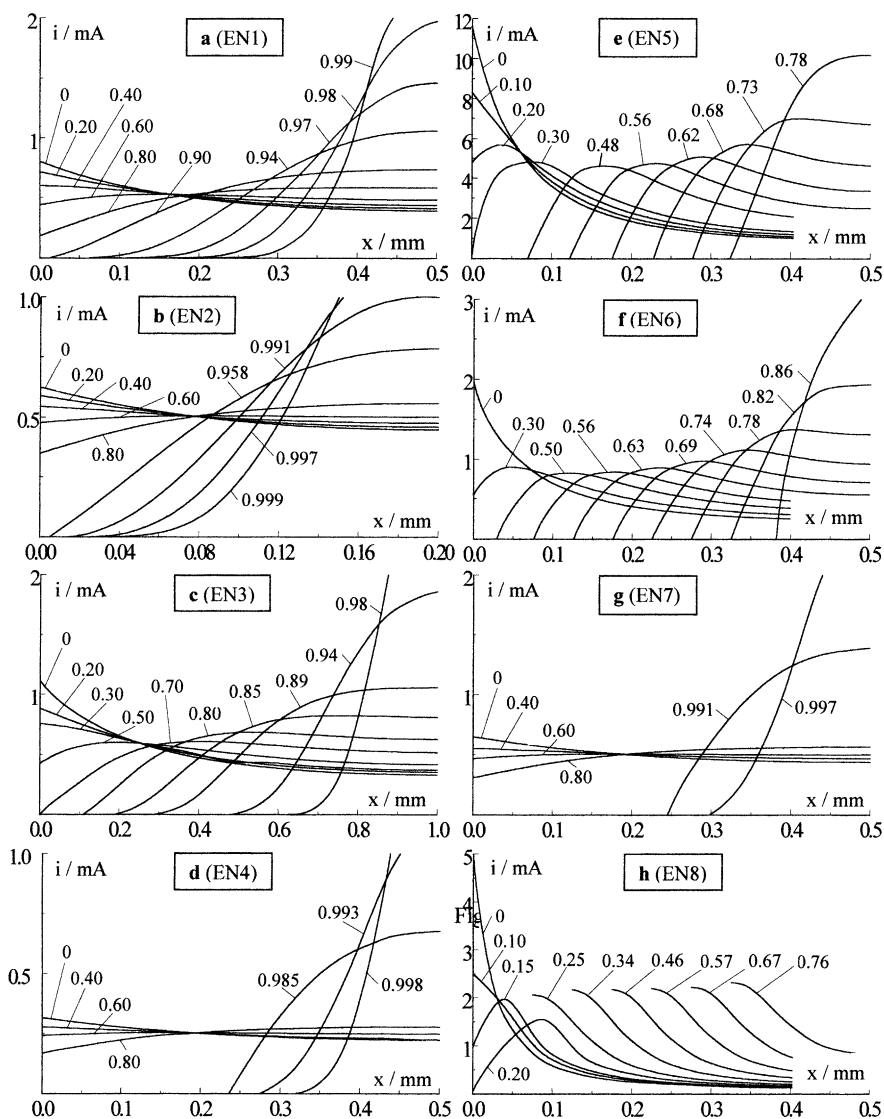
Fig. 2. Calculated current distribution throughout the thickness of the electrode. The electrode numbers (EN) are given in Table 3. The theoretical efficiencies are indicated.

the overall current density I/S (where S is the area of all silver particles) in the thin electrode is higher than in the thick one, and the polarization in the thin electrode is higher accordingly.

In Fig. 2a, f and g the dependence of current distribution on the Ag:electrolyte ratio is shown. These figures show that non-uniformity of current distribution and polarization (Fig. 3a, f and g) also decrease with increasing electrolyte
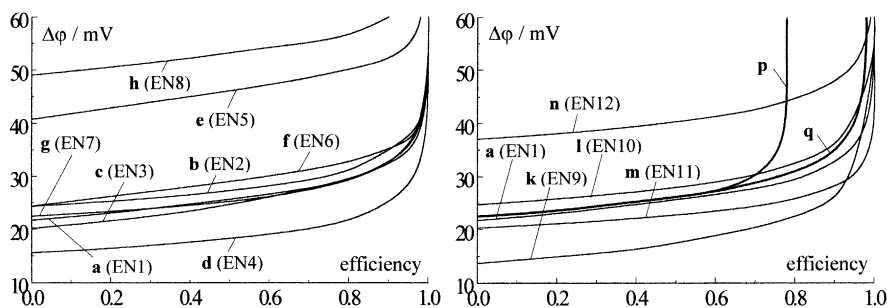

Fig. 3. Discharge curves of the electrodes. The EN for the (a–n) calculated curves are given in Table 3 p and q are the experimental curves. The explanations see in the text.

content in the electrode. It is stipulated by ionic resistance increasing as the electrode porosity decreases.

The use of an electrolyte with lower conductivity causes a sharp increase of current distribution non-uniformity (Fig. 2a and h) and electrode polarization (Fig. 3a and h). This effect is obvious, since in these conditions the ionic resistance of the electrode is increased appreciably.

The variation of the particle diameter does not change the current distribution significantly, but the electrode polarization is increased (Fig. 3a, k and l) with increasing particle diameter. It is possible to explain the last fact by the collapse of the overall area of silver particles, so increasing current density and polarization resistance.

The increase of the separator thickness does not change the current distribution, but causes increasing electrode polarization (Fig. 3a, m and n). This is obvious and does not require explanations. The experimental checking of the current distribution is difficult and was not carried out. However, the adequacy of calculations can be tested by comparison of the calculated and experimental discharge curves.

The calculated (Fig. 3a) and experimental (Fig. 3q) discharge curves of electrodes with identical compositions ($Ag:Ag_4RbI_5$ is 1:0.5) under a 10 mA overall current practically coincide in polarization, but differ considerably in efficiency (1.0 and 0.78 accordingly). As is visible in Fig. 3p, experimental efficiency increases considerably (up to 0.98) by adding carbon to the electrode material ($Ag:Ag_4RbI_5:C$ is 1:0.5:0.02).

Hence, some silver particles in experimental $Ag + Ag_4RbI_5$ electrode are isolated by electrolyte and have no electronic contact with the collector. In a $Ag + Ag_4RbI_5 + C$ electrode, the carbon bridges such particles to give electronic conduction. The good correspondence of the calculated (Fig. 3a) and experimental (Fig. 3p) discharge curves testifies to the adequacy of this model of the soluble metal electrode when applied to devices with solid electrolytes.

The results obtained allow the production of recommendations for the development of metal electrodes in devices with solid electrolytes according to the application of these devices. For example, high current density and low polarization are necessary for powerful primary batteries. Here, it is possible to recommend a thick electrode with high electrolyte content and fine silver powder.

For storage batteries, the counter electrodes of timers and other devices, in which uniform current distribution in the electrode is important, it is possible to recommend a low current density and a high proportion of electrolyte. For example, practically uniform current distribution is observed at 0.4–0.6 efficiencies with EN4 and EN7 electrodes. Therefore, for reversible electrodes, it is possible to recommend an initial discharge of such electrodes up to 0.5 efficiency, then 'discharge–charge' cycles within the limits 0.4–0.6 efficiencies.

5. Conclusions

A model of the soluble metal electrode for devices with solid electrolytes was designed. The computer simulation of electrode discharges showed that, to increase the current distribution uniformity in the electrode, it is necessary to reduce the ratio of ionic and polarization resistances in the electrode, i.e. to use high-conductivity electrolytes and metal electrodes with high polarization resistance. The good correspondence of the calculated and experimental discharge curves testifies to the adequacy of this model of the soluble metal electrode for devices with solid electrolytes.

Acknowledgements

References

[1] R.T. Foley, J. Electrochem. Soc. 116 (1969) 13C.
[2] T. Takahashi, O. Yamamoto, J. Electrochem. Soc. 117 (1970) 1.
[3] M. De Rossi, M.L. Berardelli, G. Fonseca, J. Electrochem. Soc. 120 (1973) 149.
[4] V.V. Stender, Electrochemical Production of Chlorine and Alkali, Khimteoret, Moscou, 1935 (in Russian).
[5] J. Coleman, Trans. Faraday Soc. 90 (1946) 545.
[6] V.S. Daniel-Bek, Zh.Fiz. Khim, 22 (1948) 697 (in Russian).
[7] A.N. Frumkin, Zh.Fiz. Khim, 23 (1949) 1477 (in Russian).
[8] K.-J. Euler, Naturwiss 45 (1958) 537.
[9] K.-J. Euler, Z. Elektrochem. 63 (1959) 537.
[10] K.-J. Euler, J. Appl. Electrochem. 8 (1978) 49.
[11] G.A. Korn, T.M. Korn, Mathematical Handbook for Scientists and Engineers, McGraw-Hill, New York, 1968.
[12] V.V. Skorokhod, Inzh.Fiz.Zh., 11 (1959) 51 (in Russian).
[13] A.M. Kolomoets, G.I. Ostapenko, Elektrokhimiya 16 (1980) 379 (in Russian).
[14] R.D. Armstrong, T. Dickinson, P.M. Willis, J. Electroanal. Chem. 57 (1974) 231.
[15] B.B. Owens, G.R. Argue, Science 157 (1967) 308.
[16] M.De. Rossi, G. Pistoia, B. Scrosati, J. Electrochem. Soc. 116 (1969) 1642.
[17] B.B. Owens, G.R. Argue, Science 157 (1967) 310.
[18] V.I. Layner, N.T. Kudryavtsev, Principles of Galvanization, Metallurgizdat, Moscou, 1953 (in Russian).
[19] J. Newman, Electrochemical Systems, Mir, Moscou, 1977 (in Russian).